ILETA International Information and Engineering Technology Association

Mathematical Modelling of Engineering Problems

Vol. 11, No. 6, June, 2024, pp. 1626-1632

Journal homepage: http://iieta.org/journals/mmep

Simulation Examination of the Impact of Operating Parameters on a High-Temperature Proton Exchange Membrane Fuel Cell



Kaoutar Kabouchi^{1*}, Mohamed Karim Ettouhami¹, Hamid Mounir²

- ¹ Equipe de Modélisation des Structures et Systèmes Mécaniques, ENSAM, Mohammed V University in Rabat, Rabat 10100, Morocco
- ² Research Team EMISys, Research Centre Engineering 3S, Mohammadia School of Engineers, Mohammed V University in Rabat, Rabat 11000, Morocco

Corresponding Author Email: kaoutar kabouchi@um5.ac.ma

Copyright: ©2024 The authors. This article is published by IIETA and is licensed under the CC BY 4.0 license (http://creativecommons.org/licenses/by/4.0/).

https://doi.org/10.18280/mmep.110624

Received: 7 January 2024 Revised: 11 April 2024 Accepted: 25 April 2024 Available online: 22 June 2024

Keywords:

high temperature PEM fuel cell, threedimensional model, COMSOL Multiphysics, performance, polarization curve, current density

ABSTRACT

In this research, a three-dimensional model has been developed in COMSOL Multiphysics software for numerical simulation to assess the high temperature proton exchange membrane fuel cell performance across various parameters. The results of the simulation and the data from experiments correspond closely when the values of the temperature, the thicknesses of the electrode layer and the membrane are 453.15K, 50e-6m and 100e-6m, respectively. Polarization curves at different cell temperatures, operating pressures, different porosities of gas diffusion layer, membrane conductivities, membrane thicknesses and porous electrode thicknesses are examined. The obtained results indicate that the fuel cell performance decreases when the cell runs at temperatures from 393.15K to 453.15K. Moreover, it is found that the cell performance is improved when the gas diffusion layer porosity increases from 0.1 to 0.6. Furthermore, the investigation of the fuel cell thickness membrane effect shows that a thinner membrane of 25e-6m gives the best performance. The simulation using the present developed model can be useful for optimization of the cell design and the operating conditions.

1. INTRODUCTION

Proton exchange membrane fuel cells (PEMFCs) offer a lot of potential as efficient and clean energy sources, particularly for applications in transportation and stationary power generation [1-4]. The polarization curves are commonly utilized in fuel cell performance evaluations [5-7]. In this context, fuel cell simulation is essential to understanding and optimizing the complex electrochemical processes occurring within the PEMFC [8, 9].

High-temperature PEM fuel cells (HT-PEMFCs) have garnered greater interest recently because to their potential for a variety of applications including enhanced mass transfer, simplified water management and increased tolerance for carbon monoxide (CO) poisoning [10, 11]. The temperature range in which the fuel cell stack runs is 393.15K to 473.15K [12]. As a result of the water's exclusive existence as vapor at this high operating temperature, flooding problems that occurs in low-temperature PEM fuel cells are avoided [13]. Furthermore, since it might lessen CO poisoning, it may provide a variety of fuel alternatives in the future rather than limiting fuel cell applications to the use of pure hydrogen alone [14].

In the broader context of energy technology, HT-PEMFCs represent a promising avenue for advancing the adoption of fuel cells as an efficient and clean energy conversion technology. Their improved performance, simplified operation, and broader fuel flexibility make them beneficial for a variety of applications. By addressing key limitations of conventional PEMFCs, HT-PEMFCs contribute to the advancement of sustainable energy solutions and the transition towards a low-carbon future.

The phenomena of heat transfer in HT-PEMFCs have been the subject of several experimental and numerical investigations [15-17]. Lüke et al. [18] inspected the HT-PEMFC stack performance and they asserted that the uneven current density distribution originates from oxygen reduction. Further, they contended that in fuel cells working in reformation, homogenization may be accomplished even in the absence of lowering the stack voltage during the transition from co-flow to counter-flow configuration.

Thus, durability, lifetime, and degradation of HT-PEMFCs have been emphasized and investigated [19-21]. Using a one-dimensional empirical model, Reimer et al. [22] explored the HT-PEM fuel cell's deterioration behavior.

In this work, a 3D mathematical model is constructed to inspect the HT-PEMFC performance by determining various physicochemical parameters impact on the current density. The model utilizes the Electrochemistry Module within the COMSOL Multiphysics software, contributing to understand the HT-PEMFC's internal comportment. In fact, the present paper aims to address several specific challenges related to

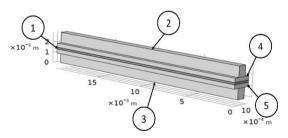
HT-PEMFCs through numerical simulation and analysis. It constitutes a novel contribution in comparison to existing models. Firstly, it focuses on assessing the HT-PEMFCs performance across various operating conditions, including different temperatures, pressures, porosities of gas diffusion layers, membrane conductivities, and thicknesses of membranes and porous electrodes. Secondly, it aims to investigate these parameters' impact on cell performance, as indicated by polarization curves. By providing insights into the complex interplay between operating parameters and cell performance, the research contributes to the HT-PEMFC design and operating conditions optimization, addressing key challenges in improving the efficiency and reliability of this promising energy conversion technology.

The article is organized as follows for the remainder of it: Section 2 provides a thorough explanation of the model developed in this study. In Section 3, we elaborate our 3D HT-PEM model implemented in COMSOL Multiphysics. Section 4 presents and discusses the obtained results of our investigation, offering a detailed analysis of the influence of temperature, pressure, GDL porosity, membrane conductivity, electrode thickness and membrane thickness on cell performance. Section 5 concludes the study, summarizes the main contributions and outlines opportunities for future research in this field.

2. MATHEMATICAL MODELING

2.1 Geometric model

The three-dimensional model of a single channel of HT-PEMFC is depicted in Figure 1. The cathode channel, cathode Gas Diffusion Layer (GDL), cathode electrode, membrane, anode electrode, anode GDL, and anode channel are the seven zones that compose the model. The geometric parameters used in the developed model are listed in Table 1.



(1: Membrane; 2: Anode Channel; 3: Cathode Channel; 4: Anode GDL; 5: Cathode GDL)

Figure 1. Three-dimensional modeling of the HT-PEMFC

Table 1. Geometrical specifications

Description	Value
Channel width	0.7874e-3m
Channel height	1e-3m
Cell length	0.02m
Rib width	0.90932e-3m
Membrane thickness	100e-6m
Porous electrode thickness	50e-6m

2.2 Basic assumptions

Assumptions such as a three-dimensional and steady model, ideal gases as inlet gases, laminar flow, incompressible fluid,

constant thermo-physical properties, an isothermal system and isotropic materials are made. The assumptions made in the model serve as simplifications to facilitate numerical simulation. The assumption of an isothermal system is justified in this study because it allows for easier modeling and analysis, especially for steady-state conditions. Since the focus is primarily on understanding the impact of different operating parameters on the HT-PEMFC performance, assuming isothermal conditions helps in isolating the effects of other parameters without introducing unnecessary complexity. Additionally, given that the temperature range studied (393.15K to 453.15K) is relatively narrow, any minor deviations from isothermal behavior are likely to have minimal impact on the overall conclusions of the study.

2.3 Governing equations

The mathematical expressions for Maxwell-Stefan, continuity, and conservation of electric charge can be recapitulated as follows [15]:

Maxwell-Stefan equation:

$$\nabla \cdot \left\{ -\rho \omega_i \sum_{j=1}^n D_{ij} \left[\frac{M}{M_j} \left(\nabla \omega_j + \omega_j \frac{\nabla M}{M} \right) + (x_j - \omega_j) \frac{\nabla P}{P} \right] + \rho \omega_i u \right\} = R_i$$
 (1)

Continuity equation:

$$\nabla(\rho u) = S \tag{2}$$

Conservation of electric charge:

$$\nabla \cdot (-\sigma_{s} \nabla \cdot \phi_{s}) = S_{s} \tag{3}$$

$$\nabla \cdot (-\sigma_m \nabla \cdot \phi_m) = S_m \tag{4}$$

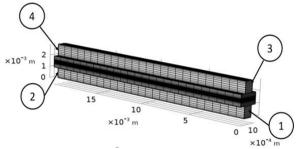
2.4 Boundary conditions

The model developed in this study is governed by several boundary conditions. These include initializing all values to zero, enforcing continuity at all internal boundaries, and applying a no-slip condition to all channel walls. In addition, in time-dependent analysis, the temperature and velocity are given at the channel inlet and are represented by a step function. In addition, the HT-PEMFC is insulated from the surrounding environment. Section "Numerical procedure" provides the specific parameter values employed in this work.

3. NUMERICAL PROCEDURE

The COMSOL software is used to create a structured grid (as shown in Figure 2) for the model geometry. There are 972 edge elements, 7392 boundary elements, and 19708 domain elements in the mesh. Boundary conditions from COMSOL and a simple procedure based on the technique of finite elements are used to solve the governing equations of Maxwell-Stefan, continuity, and conservation of electric charge, including relationships between several geometric parameters associated with the HT-PEMFC subdomains in order to speed up the convergence of the solution [23]. In addition, a method using algebraic multigrid iteration was successfully applied to solve the model's governing equations' finite element discretization. Table 2 presents the mesh characteristics used in the 3D model simulation to achieve

convergent solutions. Each layer of the HT-PEMFC model geometry depicted in Figure 1 was effectively addressed by the mesh resolutions and sizes listed in Table 2, ensuring convergent solutions across various of parameter values investigated in this study. The cell temperature, pressure, voltage are 453.15K, 1.0133e5Pa and 0.95V, respectively.



(1: Cathode inlet; 2: Cathode outlet; 3: Anode inlet; 4: Anode outlet)

Figure 2. Structure after meshing

Table 2. Mesh characteristics of the HT-PEMFC model

Mesh Characteristics	Value
Minimum element size	3.6e-4
Maximum element size	0.002
Maximum elemental growth rate	1.5
Resolution of narrow regions	0.5
Resolution of curvature	0.6

The following physicochemical parameters were used in this model:

The porosity of GDL is 0.4, the GDL permeability is $1.18e-11m^2$, the GDL electric conductivity is $222~S.m^{-1}$, the reference concentration of O_2 and H_2 is $40.88~mol.m^{-3}$, respectively. The membrane conductivity is $9.82S.m^{-1}$ and the specific surface area value is $1e7m^{-1}$. The inlet flow velocity at the anode and at the cathode are $0.10352m.s^{-1}$ and $0.41078m.s^{-1}$, respectively. The viscosity at the anode and at the cathode are 1.19e-5Pa.s and 2.46e-5Pa.s, respectively. The molar mass of H_2 , N_2 , H_2O and O_2 are $0.002kg.mol^{-1}$, $0.028kg.mol^{-1}$, $0.018kg.mol^{-1}$ and $0.032kg.mol^{-1}$, respectively. The inlet mass fraction of H_2 (anode), O_2 (cathode) and H_2O are 0.963, 0.202 and 0.037, respectively.

4. RESULTS AND DISCUSSIONS

4.1 Model verification

To affirm the validity of our model, we juxtapose the numerical findings derived from our current model with those from an experimental investigation conducted by Ubong et al. [15]. The temperature, thicknesses of the electrode layer and the membrane were identical to those in the experimental test, and they are 453.15K, 50e-6m and 100e-6m, respectively. Figure 3 shows that the experimental results and those obtained by simulation are very close with a slight difference. These discrepancies can be explained as follows:

(i) The performance of the cell in the simulation surpasses slightly that of the experiment in the low current density zone. This can be attributed to activation loss being more significant in experimental tests, as real-world gases are non-ideal. In the model, the properties of the inlet gas are held constant, while

in experiments, they could change. Additionally, the model characterizes the porous medium material without defects, whereas experimental materials often have inherent imperfections.

(ii) For safety reasons, the test of experimentation doesn't reach 0 V from the open circuit voltage, it is expected that the voltage would rapidly drop at very low voltages due to concentration loss.

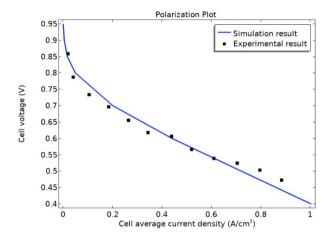


Figure 3. Comparison of current modeling results with experimental data

4.2 Simulation results

In this section, the effect of different physicochemical parameters on the HT-PEMFC performance is investigated. The PEMFC performance can be evaluated using the polarization curve which helps identify sources of losses and guide the optimization of components and operating conditions to improve the overall efficiency of the system [24].

Indeed, sensitivity analyzes serve an important part in evaluating the model robustness. These analyzes consist of evaluating how variations in input parameters affect the results of the simulation. As part of this study, sensitivity analyzes have performed by changing the values of parameters such as operating temperature, membrane and electrode thickness, membrane conductivity, etc. The simulation parameters chosen are close to those of the experiment by Ubong et al. [15]. In this section, we have discussed the results of these analyzes and have determined the most sensitive parameters which significantly influence the fuel cell performance.

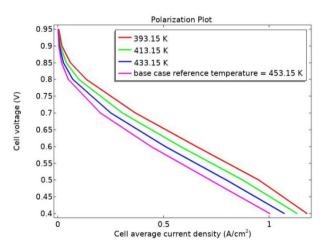


Figure 4. Polarization curves for different temperatures

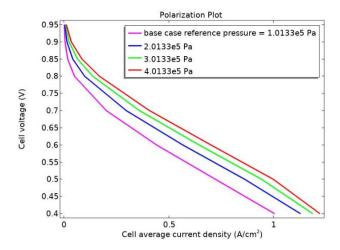


Figure 5. Polarization curves for different pressures

4.2.1 Operating temperature effect

Figure 4 shows the temperature effect on the HT-PEMFC performance characteristics. Indeed, the temperature is varied from 453.15K to 393.15K and the pressure is fixed at 1.0133e5Pa. The figure indicates that reducing the operating temperature results in enhanced fuel cell performance. The improvement is more significant in the ohmic loss section compared to the activation over potential loss section. This trend can be explained by the higher diffusivity of reactants and improved membrane conductivity at lower temperatures. Moreover, it is known that increasing the operating temperature improves the rate of electrochemical reactions as well as mass transfer of the reactants. On the other hand, increasing the temperature could result in the chemical degradation of the PEMFC leading to reduced life time of this fuel cell [25, 26].

4.2.2 Operating pressure effect

Figure 5 reports the pressure impact on the HT-PEMFC performance characteristics. The temperature is operated at 453.15K. This figure shows that the fuel cell performance increases gradually as the operating pressure ranges from 1.0133e5Pa to 4.0133e5Pa. The performance is more marked between 1.0133e5-2.0133e5Pa, but the improvement declines as pressure exceeds 2.0133e5 Pa. With the development of the HT-PEMFC, which operates at higher pressures, this improvement in fuel cell performance might lead to a new trend in PEMFC technology. The improvement of the cell performance as a result of increased operating pressure can be attributed to the increase of diffusivity of the reactant gases and consequently, the decrease of the mass transport resistance problem [27].

4.2.3 GDL porosity effect

Figure 6 shows the GDL porosity impact on the HT-PEMFC performance characteristics. Four distinct GDL porosity values are employed for the simulation: the base case value 0.4 along with 0.1, 0.2, and 0.6. As depicted in Figure 6, it is evident that higher GDL porosities lead to increased output voltages, particularly at higher cell current densities. But, the value of 0.1 gives the lowest polarisation curve. This suggests that the flow of the reactant through the GDL may be limited by the value of 0.1, resulting in a diminished ion concentration at the electrode and as a result yielding a lower polarisation curve.

On the contrary, the curves corresponding to higher GDL porosities, such as 0.4 and 0.6, closely aligned because of the unhindered reactant flow. Therefore, there is almost no significant impact of GDL porosity values of 0.4 and 0.6 on the HT-PEMFC performance curves. This highlights the importance of choosing the most suitable porosity levels for the selected GDL materials so as to improve the HT-PEMFC performance.

4.2.4 Membrane ionic conductivity effect

Figure 7 shows the membrane ionic conductivity effect on the HT-PEMFC performance characteristics. Three distinct values are considered, comprising the value in the basic case of 9.825S.m⁻¹, 19.825S.m⁻¹ and 29.825S.m⁻¹. This evaluation aims to determine the influence of the membrane ionic conductivity on the voltage versus current relationship in the HT-PEMFC. As depicted in Figure 7, increasing the membrane ionic conductivity leads to an increase in the cell voltage. As a result, the cell polarization curves shift to higher potentials with higher HT-PEMFC current density. This suggests a significant improvement in the HT-PEMFC polarization curves with the higher membrane's ionic conductivities. For example, at a current density of 1 A.cm⁻², the cell output voltage is almost 0.41V for the value of 9.825S.m⁻¹ while that of a membrane with an ionic conductivity of 29.825 S.m⁻¹ yields an output voltage of around 0.545V. This signifies a remarkable 32.92% increase in cell voltage when the ionic conductivity of the membrane is increased from 9.825 S.m⁻¹ to 29.825 S.m⁻¹, as clearly depicted in Figure 7.

4.2.5 Membrane thickness effect

Numerical simulations are conducted to examine the impact of membrane thickness on the performance characteristics. Five distinct values of thickness are considered, including 25e-6m, 50e-6m, 75e-6m, base case value of 100e-6m and 125e-6m, keeping all parameters constant. Figure 8 reports the polarization curves as a function of the membrane thickness. It is found that the optimal cell performance is achieved at a thinner thickness value of 25e-6m. This can be explained by the reduced losses, improved proton conductivity, and enhanced reactant transport, all of which contribute to the power output and overall efficiency. On the contrary, thicker membranes (>25e-6m) exhibit increased losses due to hindered reactant transport, leading to reduced cell performance. Therefore, it is crucial to optimize membrane thickness to achieve fuel cell efficiency and performance.

4.2.6 Electrode thickness effect

The fuel cell performance is evaluated by conducting analyses at porous electrode thicknesses of 30e-6m, 50e-6m, 70e-6m, and 100e-6m. The operating temperature and pressure are maintained at 453.15K and 1.0133e5Pa, respectively. The membrane has a thickness of 100e-6m.

Figure 9 illustrates the polarization achieved by the fuel cell using four electrode catalyst layer thicknesses. This figure indicates that increasing the electrode thickness results in minimal shifts upwards in the polarization curves, which is particularly evident at lower current density loads. This observation indicates that thicker electrodes, such as a thickness of 100e-6m, yield higher voltages, as shown in Figure 9. This value of thickness enhances slightly the HT-PEMFC performance within the range of low current densities, from 0.05 A.cm⁻² to 0.5 A.cm⁻². However, at higher current

densities, ranging from 0.5 A.cm⁻² to 1 A.cm⁻², the performance of the cell is not affected by the electrode thickness value.

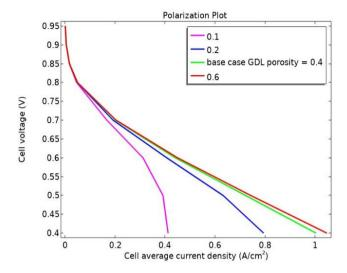


Figure 6. Polarization curves for different GDL porosities

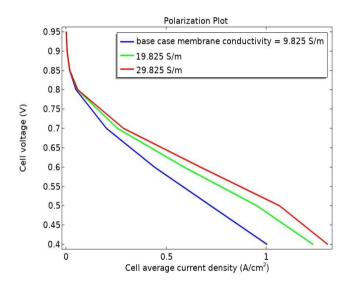


Figure 7. Polarization curves for different membrane ionic conductivities

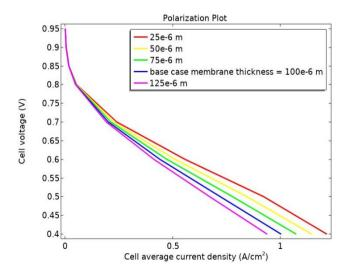


Figure 8. Polarization curves of HT-PEMFCs for different membrane thicknesses

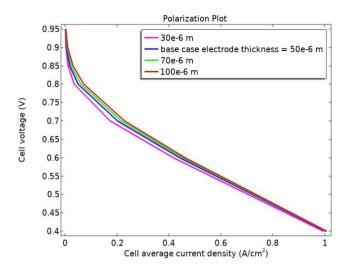


Figure 9. Polarization curves of HT-PEMFCs for different electrode catalyst layer thicknesses

5. CONCLUSIONS

A three-dimensional HT-PEMFC numerical model was developed by COMSOL Multiphysics to depict the comportment of the cell. The published data from experiments and the modeling results showed substantial convergence. Furthermore, the PEMFC performance was evaluated using the polarization curves. The impact of the operating parameters on the cell performance were investigated. This performance is discovered to be enhanced by a drop in temperature from 453.15K to 393.15K. This is due to increase of exchange current density, gas diffusivity and membrane conductivity at lower temperatures. Because of the increase in the gas diffusivities, the fuel cell performance increases when the operating pressure rises from 1.0133e5Pa to 4.0133e5Pa. Moreover, the impacts of increasing the membrane ionic conductivity and the GDL porosity on the cell performance were explored. When the thickness of the porous electrode increases from 30e-6m to 100e-6m, the cell performance advances significantly. In addition, it is suggested that a thinner membrane offers better performance investigating the fuel cell thickness membrane effect due to the less internal resistance. The insights gained from this study hold great promise for advancing diagnostic analyses and optimizing HT-PEMFC systems in the pursuit of efficient and sustainable energy conversion technologies.

In future work, the research can be expanded to uncover how both operating and design parameters influence the HT-PEMFC performance when considered together. In addition, these findings can help to determine the design and the optimal operating conditions of HTPEMFC in practical applications.

ACKNOWLEDGMENT

This work is supported by Mohammed V University in Rabat. The authors gratefully acknowledge the support.

REFERENCES

[1] Abokhalil, A.G., Alobaid, M., Makky, A.A. (2023). Innovative approaches to enhance the performance and

- durability of proton exchange membrane fuel cells. Energies, 16(14): 5572. https://doi.org/10.3390/en16145572
- [2] Li, N., Cui, X., Zhu, J., Zhou, M., Liso, V., Cinti, G., Araya, S.S. (2023). A review of reformed methanol-high temperature proton exchange membrane fuel cell systems. Renewable and Sustainable Energy Reviews, 182: 113395. https://doi.org/10.1016/j.rser.2023.113395
- [3] Zhang, Y., He, S., Jiang, X., Fang, H., Wang, Z., Cao, J., Yang, X., Li, Q. (2024). Performance evaluation on full-scale proton exchange membrane fuel cell: Mutual validation of one-dimensional, three-dimensional and experimental investigations. Energy Conversion and Management, 299: 117905. https://doi.org/10.1016/j.enconman.2023.117905
- [4] Amadane, Y., Mounir, H., Elmarjani, A., Karim, E.M. (2019). Numerical investigation of hydrogen consumption in proton exchange membrane fuel cell by using computational fluid dynamics (CFD) simulation. Mediterranean Journal of Chemistry, 7(6): 396-415. https://doi.org/10.13171/mjc7618121415ya
- [5] Tang, X., Zhang, Y., Xu, S. (2023). Experimental study of PEM fuel cell temperature characteristic and corresponding automated optimal temperature calibration model. Energy, 283: 128456. https://doi.org/10.1016/j.energy.2023.128456
- [6] Fan, L., Tu, Z., Chan, S.H. (2022). Technological and Engineering design of a megawatt proton exchange membrane fuel cell system. Energy, 257: 124728. https://doi.org/10.1016/j.energy.2022.124728
- [7] Huang, F., Qiu, D., Lan, S., Yi, P., Peng, L. (2020). Performance evaluation of commercial-size proton exchange membrane fuel cell stacks considering air flow distribution in the manifold. Energy Conversion and Management, 203: 112256. https://doi.org/10.1016/j.enconman.2019.112256
- [8] Asadzade, M., Shamloo, A. (2017). Design and simulation of a novel bipolar plate based on lung-shaped bio-inspired flow pattern for PEM fuel cell. International Journal of Energy Research, 41(12): 1730-1739. https://doi.org/10.1002/er.3741
- [9] Huang, Y., Xiao, X., Kang, H., Lv, J., Zeng, R., Shen, J. (2022). Thermal management of polymer electrolyte membrane fuel cells: A critical review of heat transfer mechanisms, cooling approaches, and advanced cooling techniques analysis. Energy Conversion and Management, 254: 115221. https://doi.org/10.1016/j.enconman.2022.115221
- [10] Chippar, P., Oh, K., Kim, D., Hong, T.W., Kim, W., Ju, H. (2013). Coupled mechanical stress and multi-dimensional CFD analysis for high temperature proton exchange membrane fuel cells (HT-PEMFCs). International Journal of Hydrogen Energy, 38(18): 7715-7724. https://doi.org/10.1016/j.ijhydene.2012.07.122
- [11] Dafalla, A.M., Liu, J., Wang, N., Abdalla, A.S., Jiang, F. (2020). Numerical simulation of high temperature PEM fuel cell performance under different key operating and design parameters. Journal of Advanced Thermal Science Research, 7: 1-10. https://doi.org/10.15377/2409-5826.2020.07.1
- [12] Zhang, C., Zhou, W., Ehteshami, M.M., Wang, Y., Chan, S.H. (2015). Determination of the optimal operating temperature range for high temperature PEM fuel cell considering its performance, CO tolerance and

- degradation. Energy Conversion and Management, 105: 433-441.
- https://doi.org/10.1016/j.enconman.2015.08.011
- [13] Sousa, T., Mamlouk, M., Scott, K. (2010). An isothermal model of a laboratory intermediate temperature fuel cell using PBI doped phosphoric acid membranes. Chemical Engineering Science, 65(8): 2513-2530. https://doi.org/10.1016/j.ces.2009.12.038
- [14] Xia, L., Zhang, C., Hu, M., Jiang, S., Chin, C.S., Gao, Z., Liao, Q. (2018). Investigation of parameter effects on the performance of high-temperature PEM fuel cell. International Journal of Hydrogen Energy, 43(52): 23441-23449. https://doi.org/10.1016/j.ijhydene.2018.10.210
- [15] Ubong, E.U., Shi, Z., Wang, X. (2009). Three-dimensional modeling and experimental study of a high temperature PBI-based PEM fuel cell. Journal of the Electrochemical Society, 156(10): B1276. https://doi.org/10.1149/1.3203309
- [16] Rasheed, R.K.A., Liao, Q., Caizhi, Z., Chan, S.H. (2017). A review on modelling of high temperature proton exchange membrane fuel cells (HT-PEMFCs). International Journal of Hydrogen Energy, 42(5): 3142-3165. https://doi.org/10.1016/j.ijhydene.2016.10.078
- [17] Rosli, R.E., Sulong, A.B., Daud, W.R.W., Zulkifley, M.A., Husaini, T., Rosli, M.I., Majlan, E.H., Haque, M.A. (2017). A review of high-temperature proton exchange membrane fuel cell (HT-PEMFC) system. International Journal of Hydrogen Energy, 42(14): 9293-9314. https://doi.org/10.1016/j.ijhydene.2016.06.211
- [18] Lüke, L., Janßen, H., Kvesić, M., Lehnert, W., Stolten, D. (2012). Performance analysis of HT-PEFC stacks. International Journal of Hydrogen Energy, 37(11): 9171-9181. https://doi.org/10.1016/j.ijhydene.2012.02.190
- [19] Salomov, U.R., Chiavazzo, E., Fasano, M., Asinari, P. (2017). Pore-and macro-scale simulations of high temperature proton exchange fuel cells-HTPEMFC-and possible strategies for enhancing durability. International Journal of Hydrogen Energy, 42(43): 26730-26743. https://doi.org/10.1016/j.ijhydene.2017.09.011
- [20] Úbeda, D., Cañizares, P., Ferreira-Aparicio, P., Chaparro, A.M., Lobato, J., Rodrigo, M.A. (2016). Life test of a high temperature PEM fuel cell prepared by electrospray. International Journal of Hydrogen Energy, 41(44): 20294-20304.
 https://doi.org/10.1016/j.iihydana.2016.00.100
 - https://doi.org/10.1016/j.ijhydene.2016.09.109
- [21] Yang, Y., Zhang, X., Guo, L., Liu, H. (2017). Degradation mitigation effects of pressure swing in proton exchange membrane fuel cells with dead-ended anode. International Journal of Hydrogen Energy, 42(38): 24435-24447. https://doi.org/10.1016/j.ijhydene.2017.07.223
- [22] Reimer, U., Schumacher, B., Lehnert, W. (2014). Accelerated degradation of high-temperature polymer electrolyte fuel cells: Discussion and empirical modeling. Journal of the Electrochemical Society, 162(1): F153. https://doi.org/10.1149/2.0961501jes
- [23] Balocco, C., Petrone, G. (2018). Heat and moisture transfer investigation of surface building materials. Mathematical Modelling of Engineering Problems, 5(3): 146-152. https://doi.org/10.18280/mmep.050303
- [24] Liu, L., Liu, T., Ding, F., Zhang, H., Zheng, J., Li, Y. (2021). Exploration of the polarization curve for proton-exchange membrane fuel cells. ACS Applied Materials

- & Interfaces, 13(49): 58838-58847. https://doi.org/10.1021/acsami.1c20289
- [25] Xu, J., Xiao, S., Xu, X., Xu, X. (2022). Numerical study of carbon monoxide poisoning effect on high temperature PEMFCs based on an elementary reaction kinetics coupled electrochemical reaction model. Applied Energy, 318: 119214. https://doi.org/10.1016/j.apenergy.2022.119214
- [26] Ren, P., Pei, P., Li, Y., Wu, Z., Chen, D., Huang, S. (2020). Degradation mechanisms of proton exchange membrane fuel cell under typical automotive operating conditions. Progress in Energy and Combustion Science, 80: 100859. https://doi.org/10.1016/j.pecs.2020.100859
- [27] Kahveci, E.E., Taymaz, I. (2018). Assessment of single-serpentine PEM fuel cell model developed by computational fluid dynamics. Fuel, 217: 51-58. https://doi.org/10.1016/j.fuel.2017.12.073

NOMENCLATURE

D diffusion coefficient
 M molecular mass, kg.mol⁻¹

- P pressure, Pa
- R source term brought on by chemical processes, kg.m⁻³
- S current source term, A.m⁻³
- u velocity vector
- x Molar fraction

Greek symbols

- φ phase potential
- σ effective electric conductivity, S.m⁻¹
- ω mass fraction
- ρ gas mixture density, kg.m⁻³
- μ dynamic viscosity, kg. m⁻¹.s⁻¹

Subscripts

- i particular species of H₂ and H₂O (anode)
- j particular species of O₂, H₂O, and N₂ (cathode)
- s solid phase
- m membrane